THE ASTROPHYSICAL JOURNAL, 322:302–314, 1987 November 1

SELECTIVE MASS LOSS, ABUNDANCE ANOMALIES, AND HELIUM-RICH STARS

G. MICHAUD, J. DUPUIS, AND G. FONTAINE
Département de Physique, Université de Montréal

AND

T. MONTMERLE
Service d'Astrophysique, Centre d'Études Nucléaires de Saclay, France
Received 1987 January 16; accepted 1987 April 22

ABSTRACT

In the presence of mass loss, the He abundance in the line-forming region is modified by the chemical separation that takes place not only in the atmospheric region but also in the wind and in the envelope. Since He-rich stars of the upper main sequence appear to be a hot extension of the Ap-Bp phenomenon in which mass loss is observed to be present, we here take diffusion in the wind, the atmosphere, and the envelope simultaneously into account in order to obtain constraints on the hydrodynamics of mass loss.

It is shown that to explain the He enrichment by separation in the atmosphere in stars of both $T_{\rm eff} = 20{,}000$ K and $T_{\rm eff} = 25{,}000$ K requires that the mass-loss rate decrease when $T_{\rm eff}$ increases. It is also shown that the mass loss allowing separation (about $3 \times 10^{-13}\ M_\odot\ {\rm yr}^{-1}$ at $T_{\rm eff} = 25{,}000$ K) is smaller than that expected from an extrapolation of the mass-loss rates observed in O stars and of that which is observed in some He-rich stars. The magnetic field seems to be required to reduce the mass-loss rate where the separation occurs. It is suggested that most of the mass loss occurs at the poles, while the chemical separation leading to He enrichment occurs at the magnetic equator where the magnetic field reduces mass loss. This explains the observed single-wave pattern of He enrichment. It also leads to an observational test of the model: the CNO abundances should be normal.

The maximum mass loss for which separation can occur in the wind is determined to be $2 \times 10^{-12}\ M_\odot\ {\rm yr}^{-1}$ in main-sequence stars and 10 times larger in white dwarfs. However, this is obtained using models for the wind region that maximize the effect of separation, and it is argued that separation in the wind could actually be much smaller. It depends in particular on the temperature in the wind region, and cold winds lead to much less separation. Separation in the atmosphere is likely to be more important than separation in the wind.

Separation in the envelope leads to *underabundances* of helium. It is, however, shown here that for mass-loss rates leading to He overabundances by chemical separation in the atmospheric region, separation in the envelope is too slow to reduce the He abundance in the atmosphere during the main-sequence life of He-rich stars.

Confirming that the separation occurs in the atmospheric region has important hydrodynamical consequences. Not only does it limit the mass-loss rate and its space distribution, but it also implies that the He convection zones do not extend into the atmosphere and that there is little, if any, overshooting into the atmosphere.

Evaluations of the separation in the atmosphere and wind of white dwarfs and sdB stars are also carried out to show the dependence on gravity.

Subject headings: diffusion — stars: abundances — stars: interiors — stars: mass loss — stars: white dwarfs

I. INTRODUCTION

Observations of the He-rich stars of the upper main sequence suggest a link between mass loss, abundance anomalies, and diffusion. The observations of Barker *et al.* (1982) show the presence of mass loss in at least some He-rich stars. The presence of magnetic fields in these stars (Borra and Landstreet 1979), and the possibility of representing their variations by an oblique rotator, strongly link them to the Ap-Bp, He-weak, and ^{3}He-enhanced stars, especially since they constitute a temperature sequence with these objects (Osmer and Peterson 1974). Radiative acceleration is, however, unable to support the He overabundance observed in their atmosphere (Michaud *et al.* 1979). Given the success of the diffusion model in explaining the abundance anomalies of the Ap-Bp stars, we are led now to consider the effect of neglected hydrodynamical processes: before mass loss had been observed on He-rich stars, Vauclair (1975) had already suggested that diffusion could lead to He overabundances in the presence of an appropriate mass-loss rate. Specifically, we will study here the constraints that chemical separation imposes on the mass-loss model and so on the possible geometries of anomalies in He-rich stars. The observed mass-loss rate and the fact that chemical separation takes place in the presence of the wind put severe constraints on where, on the surface, the wind must be leaving the star and where He must be concentrated. This will lead to predictions on expected anomalies of other elements and so to an observational test.

To establish these constraints firmly, it is, however, necessary to study all possible regions where chemical separation can take place. The separation is possible not only in the atmosphere, as studied by Vauclair (1975), but also in the wind region (above the atmosphere) or in the envelope, below the

atmosphere. Can the downward separation that occurs in the envelope cancel the effect of the accumulation in the atmosphere in the presence of mass loss? All aspects of the process will be studied in this paper.

The emphasis will be put on separation in the wind itself. Only upper limits to chemical separation in winds will be determined, since only spherically symmetric, constant-temperature wind models will be considered, and this maximizes separation for a given mass-loss rate (see § II). These limits will be used here to interpret He-rich stars, but they could be used for other objects as well. Cases with different gravities will be studied. Our aim is not only to study He-rich stars, but more generally to set limits on the potential contribution to chemical anomalies that stellar winds may lead to. In particular, what is the maximum mass-loss rate that still allows some chemical separation to take place in the wind?

This paper does not discuss the effects of diffusion on the hydrostatic structure of the outer atmosphere, as discussed in particular by Peterson and Theys (1981), or the connected question of the amplification of the radiative acceleration on He by a horizontal magnetic field (Vauclair, Hardorp, and Peterson 1979). These might be important, but they would lead to a very different model, and the observations showing the presence of mass loss justify studying first the model based on mass loss only to explain the He enrichment.

Only a brief mention of white dwarfs and sdOB stars will be made here. Observations of the $N(\mathrm{He})/N(\mathrm{H})$ ratio in those objects (Wesemael, Green, and Liebert 1985; Petre, Shipman, and Canizares 1986) suggest an interesting competition between radiative pressure, mass loss, and chemical separation. Lines of some metals have been observed to be blueshifted in some DA white dwarfs (Bruhweiler and Kondo 1983). Heber (1986) has analyzed some sdOB stars and put constraints on the mass-loss rate from the observed He abundances. While calculations in high-gravity objects will be presented here to show the effect of gravity on the separation, detailed models of white dwarfs and sdOB stars are outside the scope of this paper and will be presented elsewhere.

II. WEAK STELLAR WINDS

a) *Observations of Winds in He-rich Stars*

From the observations of Barker *et al.* (1982), there is now convincing evidence of the presence of winds in upper–main sequence He-rich stars. These authors present *IUE* spectra of a number of objects and in particular of C IV lines of the B2 V star HD 184927. The C IV doublet has blueshifted absorption components extending 4 Å from line center. It contains a large fraction of the total absorption equivalent width.

Even a rough model of the wind shows that the mass-loss rate is large enough to influence abundance anomalies. In the absence of a precise model for the wind structure, we use, to interpret the results of Barker *et al.* (1982), the model developed by Castor, Lutz, and Seaton (1981). The model features a simple wind structure with the optical depth–velocity relation obtained from Of stars. The final relation between the mass-loss rate and the measured moment of the line profile then implicitly depends on the velocity gradient used in their model. In their expression (their eq. [4.17]), the mass-loss rate is proportional to the square of the terminal velocity and inversely proportional to the number density of the level causing the absorption in the observed line. The terminal velocity can be estimated from the observed 4 Å extension of the blueshifted C IV component, leading a 1500 Å to a velocity of 800 km s^{-1}. To obtain a lower limit to the mass-loss rate, it is assumed here that all carbon is in the state causing the observed line. The mass-loss rate is also proportional to the first moment of the line profile, W_1, that is observed. From its definition by their equation (4.2), W_1 can be interpreted as the average displacement of the line, a W_1 of 0.5 implying that this displacement is, on average, midway between the rest wavelength and the wavelength corresponding to the terminal velocity of the wind. Using this interpretation and the observations of Barker *et al.* (1982), W_1 is at least 0.2. We finally used a stellar radius of $3\ R_\odot$ and obtained a mass loss of $6.5 \times 10^{-12}\ M_\odot\ \mathrm{yr}^{-1}$ using equation (4.2) of Castor, Lutz, and Seaton (1981). This is only a rough estimate: the velocity gradient used is uncertain, the line is probably saturated contrary to assumptions of the model, and not all carbon needs be in the ground state of C IV. This last approximation is probably the worst and could easily lead to an underestimate of the mass-loss rate by a factor of 10. It thus appears most unlikely that the mass-loss rate could be significantly below $5 \times 10^{-12}\ M_\odot\ \mathrm{yr}^{-1}$. This is a constraint on our wind model.

The observations of Barker *et al.* also show that the C IV line profiles vary with time, in phase with the observed magnetic field variations for this object. They suggest that the mass loss is at least partly governed by the magnetic field configuration and therefore is not spherically symmetric. *However, in our evaluation of the mass-loss rate we assumed that the average mass loss on the visible hemisphere is present on the whole surface.* In this paper, when mass-loss rates are discussed, they always refer to such an average. When mass-loss rates are calculated, they are normalized to a spherically symmetrical mass-loss rate, even if the mass loss is occurring over only part of the surface. It is usually the local mass movement that matters for the calculations of the effect of mass loss on elements separation. Some implications of nonspherically symmetric mass loss will be discussed in § V.

b) *The Example of the Solar Wind*

The solar wind is the only weak stellar wind directly observable: it has a mass-loss rate of $10^{-14}\ M_\odot\ \mathrm{yr}^{-1}$ and a velocity of 400–800 km s^{-1} at the Earth. It will be used here as a guide to physical processes that may be important in weak winds and as a measure of the uncertainty that currently affects our understanding of wind structures.

Indeed we know that the solar wind is chemically differentiated: the elements that are neutral at $T_{\mathrm{eff}} = 10^4$ K are underabundant by factors $\sim$2–3 in the wind (time-averaged *in situ* particle measurements) and in the corona (Meyer 1985). There is a controversy as to where the chemical separation occurs, the correlation with ionization potentials suggesting that it occurs at the base of the wind.

Burgi and Geiss (1986) have recently done detailed calculations of a model for chemical separation in the solar wind, including constraints coming from the electron density observed in the corona, from the fluxes of proton and helium, and from the observed charge distribution of a few elements at 1 AU. They used the observed electron density profile to infer a temperature gradient in the corona. This temperature gradient is affected by the presence of He, and it must be obtained iteratively with the solution for chemical separation in the wind.

In the model they prefer, model 4, Burgi and Geiss (1986) obtain the result that the matter arrives at 1 AU with the same

n(He)/n(H) ratio as at the base of the wind model. No net separation occurs in the wind itself. This is to be contrasted to a number of previous models where the total He separation caused by the wind was by a factor of 2 or 3 (Jokipii 1966; Delache 1967; Nakada 1969, 1970; Yeh 1970; Geiss, Hirt, and Leutwyler 1970; Cuperman and Metzler 1975; Hollweg 1981). A comparison of the Burgi and Geiss models with the others shows that the difference is caused by the different assumed temperature structure and geometry. These are not obtained from first principles but are partly obtained from detailed solar observations and partly treated as arbitrary parameters. In particular, they assume an appropriate geometry for the magnetic flux tubes. By reducing the surface from which the wind originates close to the photosphere, flux tubes increase the particle density there and so reduce the particle separation (see also Joselyn and Holzer 1978). Such effects may be present in the magnetic He-rich stars. The temperature structure used by Burgi and Geiss also reduces the separation, mainly through its effect on the friction coefficient. As can be seen from equation (14a) below, the friction coefficient is proportional to $T^{-1.5}$ and so increases as the temperature decreases close to the star in the Burgi and Geiss (1986) model. A constant-temperature model does not have this lower temperature region close to the surface and so maximizes the separation. The only chemical separation in the Burgi and Geiss model occurs close to 0.5 $R_\odot$ above the surface and modifies the coronal structure there but leads to no separation in the flux carried by the wind.

While the work of Burgi and Geiss (1986) is the most comprehensive to date, it still requires a number of assumptions about the electron density as a function of radius, flux-tube geometry, and it does not consider the heating mechanism, which is still unknown. It illustrates the limit of our understanding of such winds.

Burgi and Geiss (1986) do not explain the He enrichment of the solar wind that Delache (1967) or Hollweg (1981) explained. The separation of He is assumed to occur in the region where He is still neutral (Geiss 1982; Vauclair and Meyer 1985). They consider this the most likely site of the separation, since there appears to be a correlation between the first ionization potential and the degree of separation that an element has gone through (Meyer 1985). Those elements with low first ionization potential have normal abundances, while those with higher first ionization potentials are underabundant. This seems difficult to understand if the separation occurs in the wind itself.

Even if a given mass-loss rate allows chemical separation to occur in a wind (as in Nakada 1969, 1970, for instance), for the same mass-loss rate in the model of Burgi and Geiss (1986) there is no separation of the matter by the wind. The chemical separation that will be calculated below will neglect all fine structure included in the model of Burgi and Geiss (1986) for the solar wind, since we do not have the information needed to include it. Only upper limits to He enrichment of the visible photosphere by chemically differentiated winds can then be obtained.

III. MODEL OF A SELECTIVE STELLAR WIND

a) Adopted Structure of Weak Stellar Winds

There are two main categories of stellar winds (see, e.g., Montmerle 1984). In hot stars (O, B, Wolf-Rayet), where the mass loss is large (up to $10^{-5}\ M_\odot\ \mathrm{yr}^{-1}$) and the wind terminal velocity high (up to 3000–4000 km s^{-1}), the wind is thought to be driven by radiation. These winds are essentially cool, that is, their temperature is not believed to be much larger than $T_{\rm eff}$. The structure of these winds is often represented by a velocity law of the form

$$v = v_\infty(1 - R_*/r)^\epsilon ,$$

with $\epsilon = 1$–2, and a constant temperature. In the cooler stars, there is evidence, from X-ray and UV observations, of the presence of flares and coronae, and solar-type activity is believed to be present, presumably accompanied by a weak solar-type wind. This wind is believed to be heated and driven by the dissipation of waves from the deep convection zones below. The structure is determined by the high temperature present in the corona.

Very little is known of the structure of the wind region of He-rich stars. The terminal velocity is of the order of 800 km s^{-1} as seen in § II*a*, which is substantially below that of the hot stars mentioned above. The driving mechanism of the wind is likely to be radiation pressure. The structure of the wind is expected to be modified by the presence of magnetic fields just as in the case of the Sun (see § II*b*).

Too little is known of the structure of the wind region of He-rich stars to choose a structure with confidence. Whichever structure is chosen, it will be necessary to let some parameters vary in order to evaluate the range of potential effects that stellar winds can have on the abundances of stellar photospheres. We choose to use the simplest possible structure and generalize it to represent the range of conditions that are possible. The structure given phenomenologically by the velocity equation above is not convenient because the velocity goes to zero at the surface of the star and cannot describe the connection to the photosphere that must be made for particle transport.

We then choose to use a constant-temperature corona to give the structure of the wind. Even if the wind velocity increases to infinity, it does so very slowly, and, in practice, it gives a structure that is not very different from the velocity law given above for radiation-driven winds. The one major change is that the velocity decreases exponentially, close to the surface, instead of going to zero. Once the velocity structure of the dominant element is determined by the coronal structure, the velocity of trace elements will also be calculated using the coronal solution. The solution for trace elements is coupled to that of the dominant species by collisions. The friction coefficient is determined by the mass-loss rate and by the temperature of the corona. For a given mass-loss rate, we will generalize the coronal solution by using a different temperature for the evaluation of the friction coefficient and for the determination of the velocity structure of the wind. The separation in cool radiative winds will be so evaluated. The high coronal temperature will determine the velocity structure; the effect of temperature on the dragging of He by protons will be evaluated by using different temperatures in relating the mass-loss rate to the coupling constant. The upper limit on the separation will be determined by using the same temperature for the velocity structure and for the friction coefficient.

A simple model of a constant-temperature corona is used here to evaluate the potential chemical separation in stellar winds. In the same spirit, we simplify the calculations by considering that either H or He is a trace element. We will show that the same limits on the mass-loss rate are imposed in both cases. The effect of the perturbation of hydrogen on the He-

dominated wind will be considered in order to show when the trace-element approximation ceases to be a good approximation and what causes it to become a poor approximation. Considering more detailed intermediate cases could be done numerically, but the accuracy gain would be illusory, since the current uncertainty of the structure of mass-loss regions in such objects dominates the uncertainties of this model. We then keep to the simplest possible model that allows an evaluation of the separation in a wind region.

b) Numerical Approach

For simplicity, we consider a spherically symmetric isothermal wind made up of fully ionized hydrogen and helium. We neglect the effects of the magnetic field so that the maximum possible separation in the wind will be obtained. The hydrodynamic three-fluid conservation and momentum equations then are (Cuperman and Metzler 1975)

$$J_i = 4\pi n_i v_i r^2 = \text{constant} , \tag{1}$$

$$kT\frac{dn_i}{dr} + n_i m_i v_i \frac{dv_i}{dr} + \frac{GMm_i n_i}{r^2} - Z_i n_i E = -\sum_{j\neq i} n_i m_{ij} \nu_{ij}(v_i - v_j) , \tag{2}$$

where we will use the index 1 for protons, 2 for helium, and e for electrons. The quantity ν_{ij} is the two-body collisional frequency for momentum transfer, m_{ij} is the reduced mass, and all other terms have their usual meanings. Because v_1 and $(v_1 - v_2)$ will never turn out to be much larger than the local thermal velocities, and in keeping with the remarks made above to simplify the solution, we will use for ν_{12} the collision frequency appropriate for thermalized particles (see Cuperman and Metzler 1975). It is the same as that which appears in the diffusion equation (cf. Chapman and Cowling 1970).

Because of electrical neutrality (see, e.g., Montmerle and Michaud 1976), the Poisson equation can be replaced by

$$n_e = n_1 + 2n_2 . \tag{3}$$

The small electron mass and the large electron mobility further allow us to simplify the electron momentum equation to

$$\frac{kT}{n_e}\frac{dn_e}{dr} + eE = 0 . \tag{4}$$

All terms of equation (2) multiplied by m_e have been neglected. The momentum exchange between protons and α-particles being much more efficient than that between either protons or α-particles and electrons, it is justified to neglect all friction terms in the electron momentum equation but to include the friction term in the momentum equations of protons and α-particles. Only the momentum exchange with protons will be considered in the helium equation, and vice versa.

Writing

$$a^2 = \frac{kT}{m_1} , \tag{5a}$$

we define the dimensionless variables

$$V_i = \frac{v_i}{a} , \tag{5b}$$

$$x = \frac{ra^2}{GM} . \tag{5c}$$

The conservation equations are used to replace n_i by v_i and then V_i. The solution for a pure ionized helium wind, in which the friction term and the effects of protons on the electric field are neglected, can be easily shown to be

$$V_{20}^2 - \frac{3}{2}\ln V_{20} = 3\ln x + \frac{2}{x} - 0.818 . \tag{6}$$

If hydrogen is a trace element, the electric field is determined by α-particles and electrons, and equation (2) becomes for protons

$$V'_{10}\left(V_{10} - \frac{1}{V_{10}}\right) = \frac{4}{x} - \frac{1}{x^2} + \frac{V'_{20}}{V_{20}} + \frac{\Lambda}{V_{20}}\left(\frac{V_{20} - V_{10}}{x^2}\right) . \tag{7}$$

In equations (6) and (7), V_{20} is the dimensionless helium velocity in the pure helium solution and V_{10} is the dimensionless proton velocity. The primes indicate derivatives with respect to x. The friction coefficient, Λ, is given by

$$\Lambda = \frac{m_{12}\nu_{12}}{m_1}\frac{GMV_{20}x^2}{a^3} \tag{8}$$

Except for a small density dependence through the Coulomb logarithm (see Cuperman and Metzler 1975), Λ is a constant at a given temperature, since ν_{12} and n_2 are proportional (see also eq. [14a]).

To solve equation (7) numerically, x_1, the value of x at the critical point defined by $V_{10} = 1$, is determined by equating the right-hand side of equation (7) to zero. The corresponding quadratic equation in x_1 always has only one positive root (the physically acceptable solution). One then differentiates equation (7) with respect to x at the critical point x_1, and one obtains a quadratic equation for $V'_{10}(x_1)$:

$$2(V'_{10})^2 = -\frac{4}{x_1^2} + \frac{2}{x_1^3} + \left(\frac{V'_{20}}{V_{20}}\right)' - \frac{2\Lambda}{x_1^3} + \frac{\Lambda(V_{20}x_1^2)'}{(V_{20}x_1^2)^2} - \frac{\Lambda}{V_{20}x_1^2}V'_{10} . \tag{9}$$

There is always only one positive root giving the solution accelerating outward, which corresponds to mass outflow (the negative root corresponds to accretion). Once $V_{10}(x_1)$ and $V'_{10}(x_1)$ are known, one returns to equation (7) and integrates numerically inward and outward from the critical point to obtain V_{10} everywhere.

The solutions $V_{10}(x)$ and $V_{20}(x)$ are valid if the abundance of protons is vanishingly small, since protons modify the electric field and drag He along. We use a perturbation method to evaluate when the presence of protons substantially modifies the He solution. To first order in n_1/n_2, the electric field is given by

$$eE = -kT\left[\frac{n'_2}{n_2} + \frac{1}{2}\left(\frac{n_1}{n_2}\right)'\Big|_0\right] = -kT\left[\frac{n'_2}{n_2} + \frac{1}{2}\frac{J_1}{J_2}\left(\frac{V_{20}}{V_{10}}\right)'\right] . \tag{10}$$

Coupled with equation (2), this leads to a helium wind of flux J_2 (defined by eq. [1]) modified by a proton wind of flux J_1:

$$V'_{21}\left(4V_{21} - \frac{3}{V_{21}}\right) = \frac{6}{x} - \frac{4}{x^2} - \frac{J_1}{J_2}\left(\frac{V_{20}}{V_{10}}\right)' + \frac{J_1\Lambda}{J_2x^2}\left(1 - \frac{V_{20}}{V_{10}}\right) , \tag{11}$$

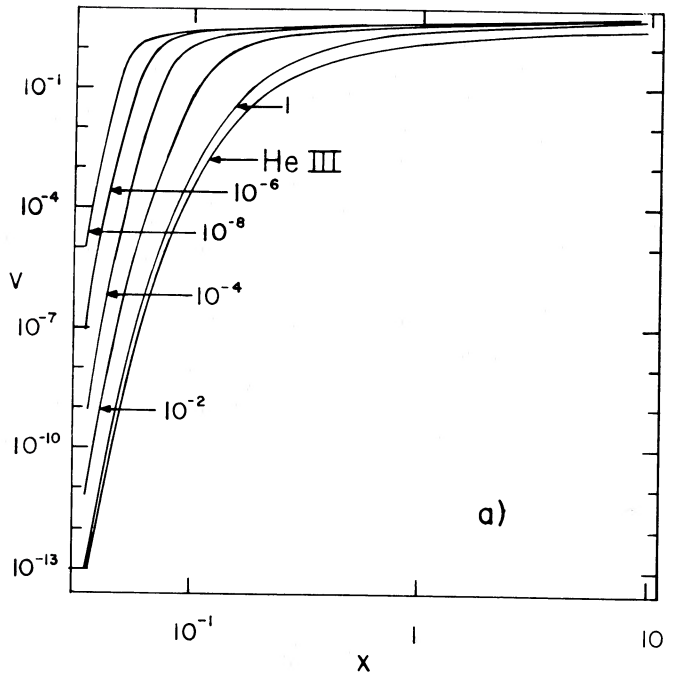

FIG. 1*a*

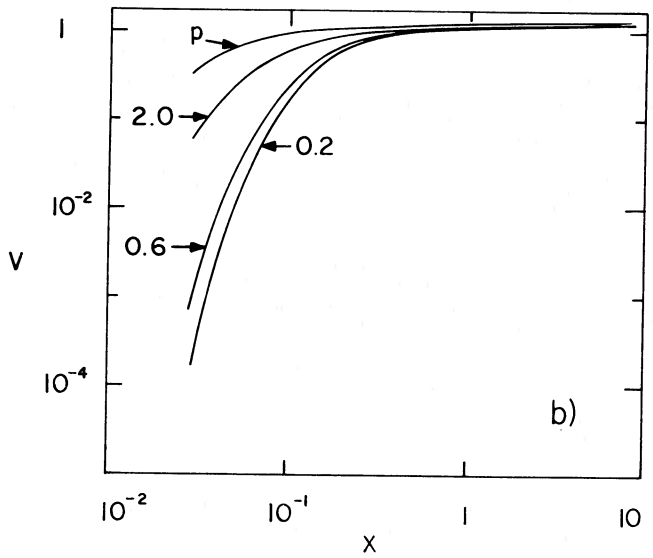

FIG. 1*b*

FIG. 1.—Coronal velocities of H and He. (*a*) Helium is the dominant species (identified by He III), and H is a trace element. (*b*) The roles are reversed; the H solution is identified by *p*. The abscissa, *x*, is a normalized distance from the center (eqs. [5*c*] and [15]), while *V* is a normalized velocity (eq. [5*b*]). The velocity of hydrogen is always the larger of the two velocities, so that helium is always left behind. When He is the dominant species, the H velocity varies with the value of Λ (eqs. [8] and [14a]), the normalized friction coefficient, which identifies the curves, but it is limited by the sound velocity. The He velocity is then independent of Λ. When hydrogen is the dominant species, the He velocity is never as large as the H velocity, but it approaches it for $\Lambda = 1$. For small values of *x*, the He velocity is very small if Δ is very small.

where $V_{21}(x)$ is the solution for the modified He wind. Equation (11) is solved numerically as described above for equation (7). When $V_{21}^2 = \frac{3}{4}$, there is a critical point at x_2, which is a solution of

$$\frac{6}{x_2} - \frac{4}{x_2^2} - \frac{J_1}{J_2}\left(\frac{V_{20}}{V_{10}}\right)' + \frac{J_1}{J_2}\frac{\Lambda}{x_2^2}\left(1 - \frac{V_{20}}{V_{10}}\right) = 0 . \quad (12)$$

The derivative of V_{21} at x_2 is obtained by differentiating equation (11),

$$8(V'_{21})^2 = -\frac{6}{x^2} + \frac{8}{x^3} - \frac{J_1}{J_2}\left(\frac{V_{20}}{V_{10}}\right)'' - \frac{2J_1\Lambda}{J_2 x^3}\left(1 - \frac{V_{20}}{V_{10}}\right) - \frac{J_1\Lambda}{J_2 x^2}\left(\frac{V_{20}}{V_{10}}\right)', \quad (13)$$

and evaluating it at x_2.

From the known values of $V_{21}(x_2)$ and $V'_{21}(x_2)$, one integrates equation (11) numerically inward and outward from the critical point. It is necessary to know $V_{10}(x)$ and its derivatives as well as $V_{20}(x)$. In contrast to V_{20}, V_{10} is not given analytically but was computed from equation (7) at some 100 points in the range $1.8 \times 10^{-2} \leq x \leq 10$ with the intervals fixed by the condition $x_i/x_{i+1} \approx$ constant. Cubic spline functions were used for the interpolation and differentiation of V_{10} in the range of interest. No numerical difficulties were encountered, and there was always only one positive root of equation (13).

c) He-*rich Winds*

We have obtained $V_{10}(x)$ and $V_{20}(x)$ for nine values of Λ in the range 10^{-8} to 1 in steps of 1 dex. This corresponds to the interesting range of Λ, since for smaller values the trend is already evident, and for larger values the solutions for protons and He III become indistinguishable. Changing Λ is equivalent to changing the mass-loss rate. For He III the relation between the two is given by

$$\Lambda = 6.6 \times 10^{22} \frac{dM/dt}{T^{3/2}M}, \quad (14a)$$

where dM/dt is in $M_\odot$ yr^{-1} and M in $M_\odot$. Figure 1*a* shows some of the solutions. Because the proton abundance is assumed small enough not to modify the helium solution (labeled He III), only the proton velocity depends on Λ. The proton solutions are labeled by the value of Λ used for them. From equation (8), Λ can be seen to be proportional to n_2, the α-particle density. The figure indicates that, for small values of *x*, the solution is inversely proportional to Λ (and so to n_2), implying that the proton velocity is determined mainly by the friction term. For small values of Λ ($\leq 10^{-4}$), the location of the critical point for protons (x_i, defined by $V_{10} = 1$) is nearly 10 times closer to the star than for He ($x_2 = \frac{2}{3}$). Numerically, between the star and x_1, the He abundance gradient, $d \ln n_2/dr$, is nearly equal to the hydrostatic gradient. This implies that in the region where protons are accelerated, the hydrostatic solution dominates for He, while the proton velocity is collision-limited. Until they reach their critical velocity (or very nearly so), protons have a relative velocity determined only by the He abundance (itself consistent with the hydrostatic equilibrium gradients). Therefore, the rapid proton acceleration can be traced back to the electric field present in the helium-dominated region. The electric field needed to prevent electrons and α-particles from separating leads to a net force

TABLE 1

DEPARTURE FROM THE PURE HELIUM SOLUTION

Λ	J_1/J_2	x_2	$\left.\frac{(V_{21}-V_{20})}{V_{20}}\right\|_{max}$
10^{-4}.....	0.0	0.666667	10^{-3}
	10^{-6}	0.666667	10^{-3}
	10^{-5}	0.666667	10^{-3}
	10^{-4}	0.666668	10^{-3}
	10^{-3}	0.666685	10^{-3}
	10^{-2}	0.666849	0.0007
	10^{-1}	0.668491	0.0069
	1	0.685050	0.068
	3	0.723715	0.20
	10	0.877643	0.54
	30	1.46968	0.93
10^{-3}.....	10^{-2}	0.666856	0.0007
	10^{-1}	0.668529	0.0071
	1	0.685358	0.071
	3	0.724753	0.20
10^{-2}.....	10^{-1}	0.668450	0.0065
	1	0.684638	0.064
	3	0.722050	0.17
	10	0.866957	0.52
10^{-1}.....	10^{-3}	0.666173	−0.0016
	10^{-2}	0.666732	−0.016
	10^{-1}	0.667322	−0.18
	1	0.673298	−4.0

(electrical plus gravitational) directed outward on protons (Montmerle and Michaud 1976). If Λ is small enough, the outward-directed relative velocity is large and the critical point is reached for small values of x.

The total separation factor caused by the wind is given by the ratio of the velocities of He and H at the base of the wind, since this measures, for a given abundance, the flux of the two species. That is,

$$\frac{1}{\beta} = \left.\frac{V_{10}}{V_{20}}\right|_{base} . \tag{14b}$$

From Figure 1*a* we find that the wind is enriched by a factor of $\sim 10^4$ if $\Lambda \sim 10^{-4}$. This enrichment is directly related to the proton critical point being closer to the surface than the critical point for helium. The exponential, nearly hydrostatic abundance gradient persists over a smaller distance for protons than for α-particles, thus reducing the relative He III abundance.

We have investigated the effects of protons on the He III wind by comparing the pure helium solution, V_{20}, obtained from equation (6) and the modified solution, V_{21}, obtained from equation (11). For four values of the friction coefficient Λ (10^{-4}, 10^{-3}, 10^{-2}, 10^{-1}), we have computed V_{21} by introducing finite proton abundances parameterized by the flux ratio J_1/J_2 (for 11 values from 0 to 30). Table 1 summarizes some of our results as a function of Λ and J_1/J_2. It can be seen that for all the values of Λ considered, the position of the He III critical point, x_2, is affected by less than 1% if $J_1/J_2 < 1$. For larger values of the flux ratio, protons can displace the He III critical point substantially outward and so modify the He III solution. Table 1 also shows the *maximum* fractional difference between the two approximations for V_2 in the range $0.018 \leq x \leq 10$. This maximum deviation is less than 1% if $J_1/J_2 < 0.1$ for all values of the friction coefficient smaller than or equal to 10^{-2}. Furthermore, for the electric field, it is the logarithmic derivative of the velocity that matters, and the differences between V'_{21}/V_{21} and V'_{20}/V_{20} are even smaller than the differences between the velocities. For $J_1/J_2 = 1$ and $\Lambda = 10^{-2}$, the difference between V'_{21}/V_{20} is only 2%. For the largest value of the friction coefficient considered here ($\Lambda = 0.1$), a detailed examination indicates that the modification to the pure He solution is, in this case, qualitatively different from that for the smaller Λ solutions. Whereas for $\Lambda \leq 10^{-2}$ the modifications due to J_1 in equation (11) are caused mainly by the correction to the electric field, for $\Lambda = 0.1$ the corrections are due mainly to the friction term. When the friction term dominates the solution, the He III velocity is increased to become very nearly equal to the proton velocity. The drag term is more important for small values of x, where the density is larger. When the corrections originate from the electric field, the He III velocity is much less affected and remains substantially different from the proton velocity. We conclude that our evaluation of the separation factors is not substantially modified if $\Lambda \lesssim 10^{-2}$ and $J_1/J_2 \lesssim 0.1$.

d) H-*rich Winds*

The solution for H-rich winds was obtained as in the case of He-rich winds, and the details of the calculations will not be repeated. Only the results will be described. In Figure 1*b* are shown particle velocities for ionized H (identified by *p*) and He (identified by the value of Λ used) when H is the dominant species. The H velocity does not vary with the friction coefficient Λ, since the He abundance is assumed to be small. Only the solution for He depends on Λ. When the friction coefficient is small enough ($\Lambda < 4$), He is not dragged by the outflowing H, and He is left behind. The He outflowing velocity is then smaller than the H velocity by large factors, leading to large enhancements of He in the atmosphere. In comparison with the He-rich case, it should be noted that the trace-element velocity is now smaller than that of the main gas, whereas the reverse is true in the He-rich case.

In Figure 2 is shown the separation factor in the wind as a function of the mass-loss rate for a main-sequence star of 25,000 K and a coronal temperature of 3×10^6 K. If the temperature is more than a factor of 3 larger than this value, the critical point is inside the stellar atmosphere (for $R = 7\,R_\odot$), as can be easily calculated using the relation between radius and the dimensionless parameter x:

$$r = 1.6 \times 10^{18}\,\frac{xM}{T}\,, \tag{15}$$

where r is in centimeters and M in solar mass units, while T is the coronal temperature. If the temperature is smaller than 10^6 K, the value of the density (at the boundary between the corona and the atmosphere) that would be needed to maintain the required mass-loss flux is larger than stellar atmosphere densities where lines form.

Figure 2*a* shows the separation factor for the case of a He-rich corona with hydrogen a trace element, while Figure 2*b* shows the case with the roles reversed, a H-rich corona and He as a trace element. Whether He or H is the dominant element, the separation is very large for mass-loss rates smaller than $2 \times 10^{-12}\,M_\odot\ \mathrm{yr}^{-1}$. Above that value, hardly any separation takes place, while below that value large separation occurs in both cases. *The maximum mass-loss rate allowing element separation does not depend sensitively on composition.* What does, however, depend on which species dominates is how the

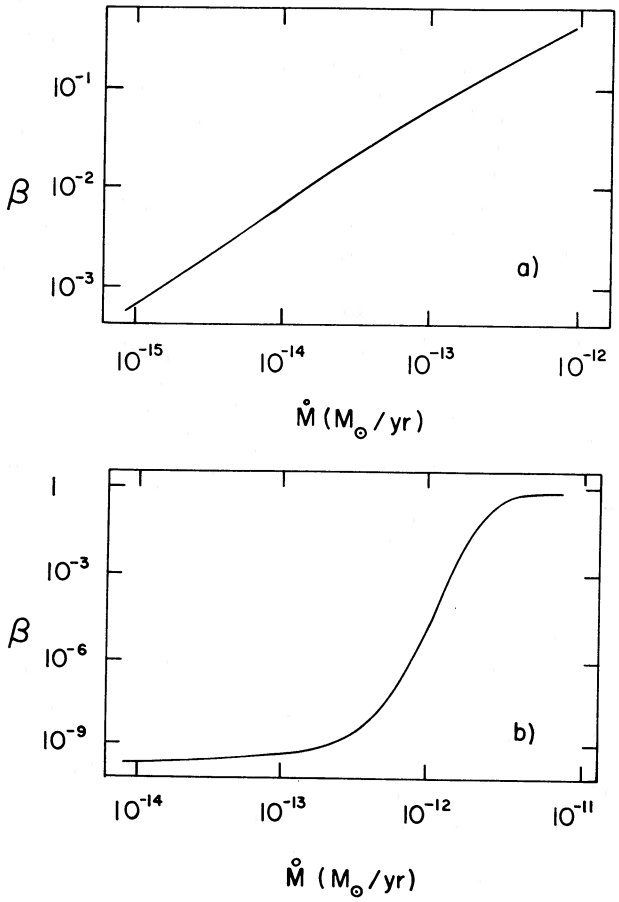

FIG. 2.—Separation factor β (eq. [14b]) as a function of the mass-loss rate in both a He-dominated corona (*a*) and a H-dominated corona (*b*). The separation factor becomes much smaller than unity for mass-loss slightly smaller than 10^{-12} $M_\odot$ yr^{-1} in both cases. The calculations were carried out for a 25,000 K main-sequence star and a 3×10^6 K corona in both cases. For small mass-loss rates, the separation is much larger in the H-dominated corona, since He is completely left behind by H in that case, while in constant-temperature coronae, both H and He leave in the He-rich case.

separation factor varies with mass loss. It varies much more rapidly when hydrogen is the dominant species. This can be understood from Figure 1. When He is the dominant species, the separation factor comes from the larger velocity of H close to the convection zone. This is limited, since the hydrogen velocity, V_{10}, must remain substantially below unity if the H wind velocity is to be smaller than the sound velocity in the photosphere. If H is the dominant species, the He velocity is proportional to the amount of He that is dragged along by H as it leaves the star. This can be very small, and the separation factor increases much more in this case than in the other.

Figure 3 shows the separation factor in the wind as a function of the mass-loss rate in a H-rich white dwarf. The coronal temperature was chosen to be 10^8 K. If it were smaller by a factor of more than 1.5, the abundance needed in the atmosphere (at the boundary between the atmosphere and the corona) to maintain the mass-loss rate would be larger than white dwarf atmosphere abundances, while if the temperature were larger by more than a factor of 2.5, the hydrogen critical point would be inside the atmosphere. The maximum mass-loss rate allowing chemical separation in the atmosphere is about 3×10^{-11} $M_\odot$ yr^{-1}, which is a factor of 10 larger than for main-sequence stars. If the corona were 2.5 times hotter, the mass-loss rate could be as large as 10^{-10} $M_\odot$ yr^{-1} and still allow significant separation. If high-gravity stars have stellar wind, these could be differentiated for larger mass-loss rates than low-gravity stars. It should, however, be noted that the higher mass-loss rates are inconsistent with models of the lower effective temperature white dwarfs. The density in the line-forming region of white dwarfs is about $\rho = 3 \times 10^{-8}$ g cm^{-3} (Wesemael *et al.* 1980). By applying the condition that pressure be continuous at the boundary between the corona and the photosphere, we obtained the result that, for the $T_{\rm eff} = 10^4$ K model, the density would need to be 4×10^{-7} g cm^{-3} at the photosphere-wind boundary to allow a mass-loss rate of 4×10^{-11} $M_\odot$ yr^{-1}. This is 10 times larger than the atmospheric density where the lines form and would imply coronal temperatures in the line forming region. Such a large mass-loss rate is then possible only in white dwarfs with $T_{\rm eff} > 10^5$ K.

IV. CONSTRAINTS ON MASS-LOSS RATES FROM HELIUM ABUNDANCES

a) Link with the Atmosphere and the Envelope

The simplest model leading to He overabundances assumes that the star is losing mass at a constant rate and that the mass loss has spherical symmetry. The chemical separation in the atmosphere and the envelope can be calculated using the diffusion velocity (see, e.g., Pelletier *et al.* 1986) along with the mass conservation equation of the dominant species in the presence of mass loss:

$$\frac{dM}{dt} = -4\pi R^2 N_{\rm H} m_p v_w \,. \tag{16}$$

Here hydrogen is assumed to be the main element leaving the star, and v_w is the mass outflow velocity in the atmosphere and the envelope. The atmosphere and envelope are assumed time-independent, but matter must flow through them at the velocity v_w to replenish what leaves through the wind. In order to simplify the argumentation, we neglect, in this discussion, the

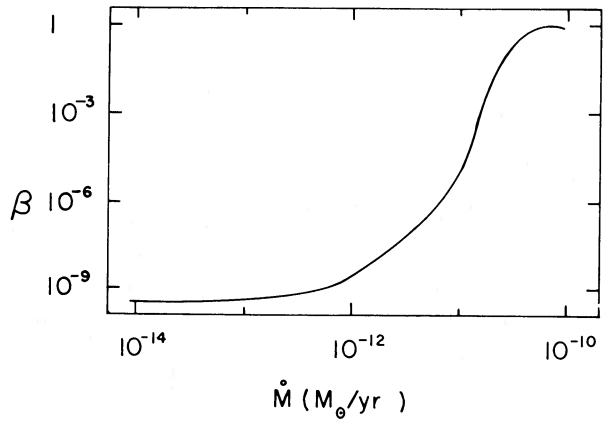

FIG. 3.—Separation factor as a function of mass loss in a 10,000 K white dwarf with a 10^8 K corona. The separation factor becomes much smaller than unity for mass-loss rates slightly smaller than 10^{-10} $M_\odot$ yr^{-1}, 2 orders of magnitude larger than in the case of main-sequence stars (see Fig. 2).

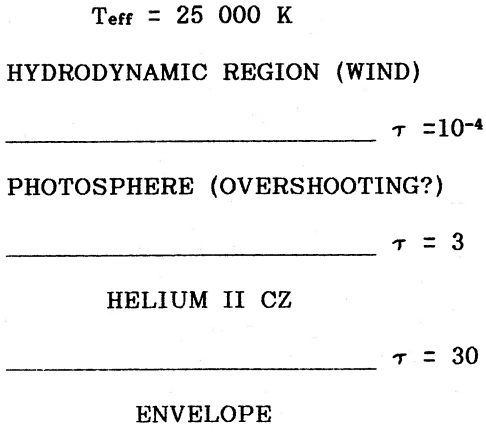

FIG. 4.—Outer structure of a 25,000 K main-sequence star. The chemical separation can take place in three regions: the envelope, the atmosphere, and the dynamical or wind region. Two of them are separated by a convection zone.

fact that He is not a test element. Taking it into account would substantially modify the equilibrium He abundances obtained but not whether overabundances appear or the time scale to establish overabundances, which are the problems discussed in this paper.

The diffusing element of concentration c [$c = N(A)/N_H$] must also satisfy a conservation equation:

$$\nabla[cN_H(v_w + v_D)] = -N_H \frac{\partial c}{\partial t}. \quad (17)$$

Note that the diffusion velocity may be as high as the wind velocity, v_w, itself. To calculate the chemical separation, it is convenient to separate the star into three zones (see Fig. 4): the coronal-wind region, the photospheric region, and the envelope region. The frontier of each of these zones is somewhat arbitrary. For the corona, one can fix where the hydrostatic solution stops being accurate; for this reason we also call it the wind region, even though the outward movement caused by the wind pervades the whole photosphere and envelope albeit with negligible dynamic effects. This definition applies even to stars that would have a cool wind and so no proper corona. At the boundary between the atmosphere and the corona, partial pressures are assumed continuous, but temperature is taken to vary suddenly without any extended transition region. For the envelope we choose the bottom of the He II convection zone for a normal He abundance as a convenient boundary.

Two models will be considered. In the first (§ IV*b*), it is assumed that the He convection zone extends into the line-forming region so that no element separation is possible in the atmosphere. The separation can then go on in the wind region and in the envelope. In the second (§ IV*d*), it will be assumed, following Vauclair (1975), that the separation goes on in the atmosphere. It then has to be assumed that convection zones lead to no overshooting or that magnetic fields stabilize the atmospheric region. The effect of the separation in the envelope will also be taken into account. Limits to the mass-loss rates that permit He overabundances will be determined in both cases. The effect of changing the temperature of the wind will be discussed in § IV*c*, while that of changing the gravity of the star will be discussed in § IV*e*.

b) Mixed Atmosphere Model

The calculations of the separation in the wind were presented in § III. The separation in the envelope was calculated as described in Michaud and Charland (1986). The flux of He arriving in the convection zone is determined from the separation that goes on in the deep envelope. We first assume that the wind is not differentiated, that is, that it carries the same hydrogen-to-helium abundance ratio as in the atmosphere. Separation in the envelope leads, for a 25,000 K star, to the time-dependent abundance variation of the He concentration in the convection zone shown in Figure 5. For mass-loss rates

TABLE 2

SETTLING TIME SCALE OF He[a]

dM/dt ($M_\odot$ yr^{-1})	τ (yr)
10^{-14}	2.0×10^6
3×10^{-14}	10^7
3×10^{-13}	3.0×10^8
10^{-12}	1.5×10^9

[a] Time scale for the helium abundance to decrease by a factor of 3 in the convection zone. T_{eff} = 18,000 K.

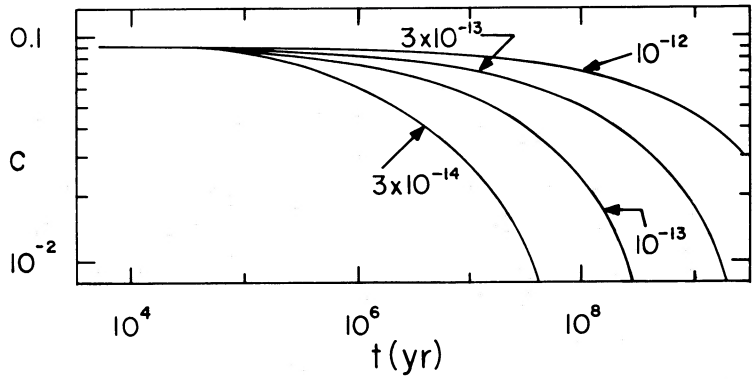

FIG. 5.—Time dependence of the He abundance in the atmosphere and convection zone of a 20,000 K main-sequence star in the presence of various mass-loss rates. The curves are identified by the mass-loss rate in $M_\odot$ yr^{-1}. The mass loss is here assumed *not* to be selective, that is, the wind is assumed to leave with the abundance of He at its base. Underabundances appear in the atmosphere within the main-sequence lifetime for mass-loss rates of 3×10^{-14} $M_\odot$ yr^{-1} and smaller.

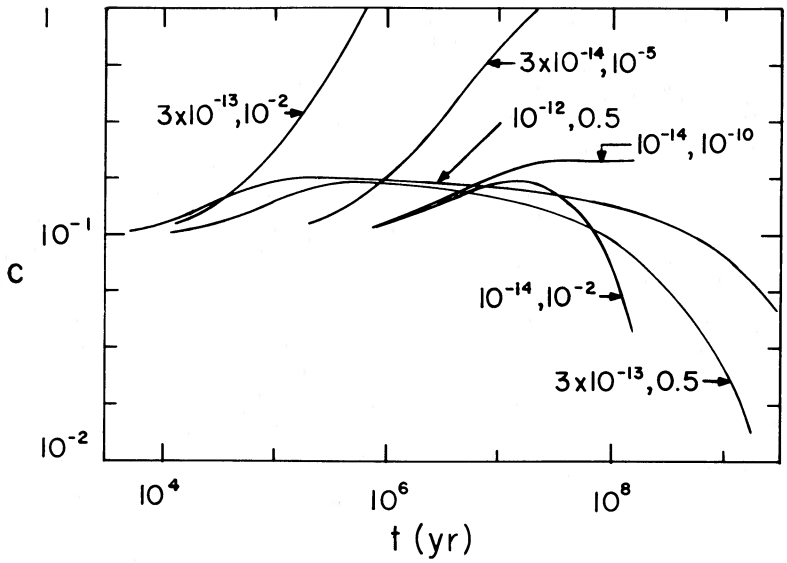

FIG. 6.—Time dependence of the He abundance in the atmosphere and convection zone of a 25,000 K main-sequence star in the presence of selective mass loss. Each curve is identified by both the mass-loss rate and the separation factor β. The maximum separation factor for a given mass-loss rate is given by Fig. 2. The He enrichment is assumed to be the same throughout the atmosphere and convection zone. The time scale to develop the He enrichment is short compared with the main-sequence lifetime. He enrichment by selective mass loss is possible within the range $10^{-14} < dM/dt < 10^{-12}\ M_\odot\ \mathrm{yr}^{-1}$. For larger mass-loss rates, no separation occurs in the wind. For smaller mass-loss rates, He sinks from the atmosphere and overabundances are not maintained even if no He leaves with the wind. As can be seen for the case $dM/dt = 3 \times 10^{-13}\ M_\odot\ \mathrm{yr}^{-1}$, the separation in the wind determines whether a given mass-loss rate leads to He overabundances or not.

of $10^{-12}\ M_\odot\ \mathrm{yr}^{-1}$ the separation becomes large only after 10^9 yr, longer than the main-sequence lifetime of such a star. Only for mass-loss rates smaller than $3 \times 10^{-14}\ M_\odot\ \mathrm{yr}^{-1}$ is the He abundance reduced by a factor of 3 within 10^7 yr (Table 2). A detailed discussion of how the separation proceeds in the envelope in the presence of mass loss may be found in Michaud and Charland (1986). In the presence of a large enough mass loss, no separation may occur immediately below the convection zone because the mass-loss velocity is larger than the diffusion velocity there. However, because for He the ratio of the diffusion to the mass-loss velocity goes as $T^{1.5}$ (see, e.g., Michaud and Charland 1986), the two velocities become equal somewhere in the envelope, and the He abundance starts to decrease when the matter appearing in the atmosphere was originally where the diffusion velocity is larger than the mass-loss velocity. In these calculations, the radiative acceleration on He is neglected. This is justified insofar as the radiative acceleration starts being important only when the He abundance has been reduced by more than a factor of 0.1 (Michaud *et al.* 1979). However, the He diffusion time scale would be increased by some 20% by radiative acceleration.

In Figure 6 are shown similar results, but for differentiated winds. The flux arriving in the convection zone is the same as that calculated for undifferentiated winds, but the wind is here assumed to carry only a fraction β (eq. [14b]) of the He in the atmosphere. This fraction β was calculated for different cases in § III and shown as a function of mass-loss rates in Figures 2 and 3. Whereas undifferentiated winds always lead to underabundances of He, differentiated winds lead to He-rich convection zones in time scales short compared with the

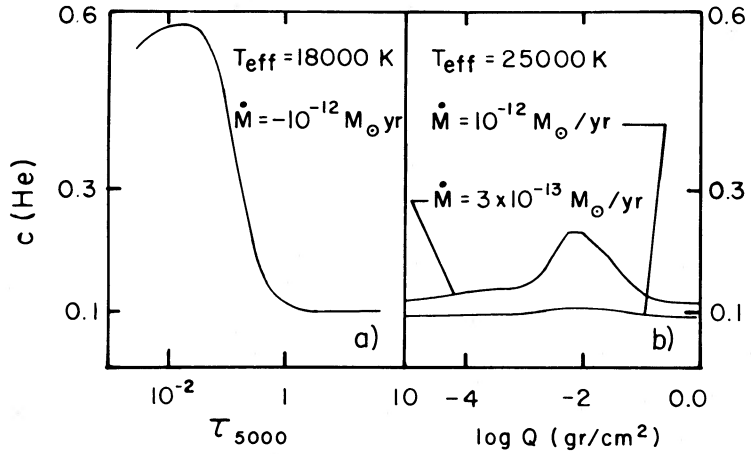

FIG. 7.—Abundance of He in the atmosphere of an 18,000 K and a 25,000 K star (log g = 4) for appropriate mass-loss rates. The 18,000 K model is from Mihalas (1965), and the 25,000 K model is from Mihalas (1972) with Q the mass in a column above the point of interest. Because of higher ionization, the mass loss must be smaller in the hotter star for overabundances to materialize.

main-sequence lifetime of these stars *if* the mass-loss rate is within the range $10^{-14} \leq dM/dt \leq 2 \times 10^{-12}\ M_\odot\ \mathrm{yr}^{-1}$. As discussed above, the upper limit results from assuming a wind structure that maximizes the separation in the wind. This shows the maximum possible range of mass-loss that may lead to He overabundances in the atmosphere from separation in the wind. A more realistic wind structure would lead to a smaller upper limit. Given our discussion of the separation of elements in the solar wind (see § II), a more realistic upper limit when He is ionized in the atmosphere would be $2 \times 10^{-13}\ M_\odot\ \mathrm{yr}^{-1}$.

This remains an upper limit, since additional sources of friction are probably present in stellar winds (Castor 1986). Instabilities are thought to develop in radiatively driven winds, leading in particular to shock-induced X-ray emission (Lucy and White 1980; Lucy 1982; Cesarsky and Montmerle 1983; White 1985). They would simultaneously create turbulence that would inhibit chemical separation. It is impossible to evaluate realistically how efficient that mixing would be. Magnetic fields may also be present in the outflowing matter, and even very small ones would inhibit the separation. Since the only coupling included is that due to atomic collisions (via the diffusion coefficient), it is a minimum coupling and the separation could be much smaller than that calculated here.

c) *Hot and Cold Winds*

As discussed in § II*a*, there is considerable uncertainty as to the structure of the winds, and, in particular, it is possible that the winds in main-sequence He-rich stars are driven by radiation and are of approximately the same temperature as the effective temperature of the star. For any appreciable wind to materialize, it has been seen that the temperature that determines the velocity-radius relation must be about 3×10^6 K in a corona. This is 100 times larger than the effective temperature. To evaluate what effect this can have on the separation, consider the temperature dependence of equation (14a). Reducing the temperature by a factor of 100 increases the friction coefficient Λ by a factor of 1000 for a given mass-loss rate. Since, for a given velocity-radius structure, it is the value of Λ that determines β, the separation factor, using a low-temperature wind reduces the critical mass-loss, allowing separation in the wind. If a temperature of 30,000 K is used in equation (14a), the critical mass-loss rate becomes $10^{-15}\ M_\odot\ \mathrm{yr}^{-1}$, while it is $10^{-12}\ M_\odot\ \mathrm{yr}^{-1}$ when the coronal temperature is used to evaluate the separation factor. Because He would be only singly ionized in a cool wind and the Coulomb collision cross section varies as Z^2, the critical mass-loss rate becomes $4 \times 10^{-15}\ M_\odot\ \mathrm{yr}^{-1}$.

Clearly, the type of wind strongly modifies the separation that can occur in it. Because of the T-dependence of equation (14a), the coronal solutions discussed in § IV*b* lead to the maximum possible separation in winds. Using the same coronal structure but a lower T in the coupling constant, the evaluation is clearly only a rough estimate of the effect of changing the wind temperature. Given the uncertainty as to the effect of magnetic fields and of the presence of transition regions, it does not appear justified to investigate other wind structures. It does appear, however, that even in the absence of additional coupling by turbulence or by magnetic fields, the limiting mass-loss rates allowing chemical separation to occur may be 2–3 orders of magnitude smaller than those given by Figures 2 and 3.

For cool winds, one should then use the curves in Figure 6 labeled 10^{-14} or 10^{-2}, or curves implying even less separation in the wind. It becomes marginal whether separation in the wind can lead to He-rich stars. Even for a mass-loss rate of $10^{-14}\ M_\odot\ \mathrm{yr}^{-1}$ and a separation factor of 10^{-2}, the atmosphere becomes marginally He-rich and remains so for barely the main-sequence lifetime. Whether separation in a wind can lead to He-rich stars depends in a sensitive way on the temperature that determines the collisions and so the separation.

d) *Stable Atmosphere Model*

To separate diffusion in the wind clearly from that in the atmosphere, it is here assumed that the separation occurs in the atmosphere, which is assumed to be stable. The model is the same as suggested by Vauclair (1975, 1981) but the calculations are carried out differently. Because we are mainly interested in establishing upper limits to the mass-loss rate, we here assume that a steady condition has been reached in which as much He arrives from the interior as leaves by the undifferentiated wind. The continuity equation (17) then applies, and the rich-hand term can be taken equal to zero as soon as the steady state is reached. The conservation equation becomes

$$N_{\mathrm{H}}\, c(v_w + v_D) = \phi\ , \tag{18}$$

where ϕ is the He flux arriving from the envelope. Using, for instance, the model atmospheres of Mihalas (1972), it is a simple matter to calculate v_w using equation (16). As the maximum mass-loss rates allowing separation to go on are approached, only small enrichments are possible in the atmosphere, and it is easy to verify that the abundance gradient plays a small role in the diffusion velocity equation. It can be neglected, and it is then a simple matter to determine v_D. The abundance profile is then obtained using equation (18). Results are shown in Figure 7. Since v_w and v_D have opposite signs, the He concentration becomes appreciable when the two velocities are about equal in magnitude. The abundance increase then compensates for the drop in the outward transport velocity. According to Figure 7, helium starts concentrating in the atmosphere for a mass-loss rate of $10^{-12}\ M_\odot\ \mathrm{yr}^{-1}$ if $T_{\mathrm{eff}} =$ 18,000 K but for a mass-loss rate of $3 \times 10^{-13}\ M_\odot\ \mathrm{yr}^{-1}$ at $T_{\mathrm{eff}} = 25{,}000$ K. This temperature dependence can be understood from the temperature dependence of the ionization of He (see Table 3). In the lower temperature model, He is nearly completely neutral, while it is nearly completely ionized in the hotter model. Since the diffusion coefficient of neutral He is some 100 times larger than that of ionized He, the mass-loss rate is larger in the cooler model. Note that these calculations were done with the diffusion coefficients of Michaud, Martel, and Ratel (1978), which should be more accurate than those used by Vauclair (1975) because they use a more realistic polarization potential to represent the interaction between protons and He. They are 4–6 times smaller than those based on the hard-sphere approximation used by Vauclair (1975).

e) *Separation in the Atmosphere of White Dwarfs and sdOB Stars*

To evaluate the separation in other types of stars, similar calculations to those described in § IV*d* have also been carried out in the atmospheres of H-rich white dwarfs (Wesemael *et al.* 1980) and of sdOB stars. The model atmospheres were kindly communicated to us by Dr. F. Wesemael. They were carried

TABLE 3

MAXIMUM VALUE OF N(He I)/N(He)[a]

$T_{\rm eff}$ (K)	N(He I)/N(He)	$T_{\rm eff}$ (K)	N(He I)/N(He)
17,500.....	1.0	25,000.....	0.1
20,000.....	0.8	27,000.....	0.014
22,500.....	0.4	30,000.....	0.0013

[a] From Mihalas 1972.

out in 0.7 $M_\odot$ white dwarfs within the temperature range 20,000–70,000 K and in sdOB stars within the range 20,000–50,000 K. The results were very similar as presented above for main-sequence stars, except that the critical mass-loss rate is reduced by a factor of about 10 in both white dwarfs and sdOB stars. At 20,000 and 25,000 K the critical mass-loss rate is $10^{-13}\ M_\odot\ {\rm yr}^{-1}$ in both cases, while it is progressively reduced to $10^{-15}\ M_\odot\ {\rm yr}^{-1}$ as the temperature is further increased and He is completely ionized. This can be easily understood using equation (14a). The masses used here are about 10 times smaller than those of main-sequence He-rich stars. For a given value of a critical friction coefficient, the mass-loss rate must be reduced by the same factor.

The implications for the mass-loss rates of those white dwarfs and sdOB stars that are observed to have experienced some chemical separation of H and He will be presented elsewhere.

V. MODELS FOR HELIUM-RICH STARS: CONSTRAINTS FROM DIFFUSION

On the one hand, according to the conclusions of § II, a mass-loss rate of at least $5 \times 10^{-12}\ M_\odot\ {\rm yr}^{-1}$ is needed to explain the anisotropy of the C IV lines, observed on main-sequence He-rich stars. On the other hand, according to the results of § IV, the maximum mass-loss rate that can lead to an He enrichment through element separation is $10^{-12}\ M_\odot\ {\rm yr}^{-1}$. This excludes, in at least some of the He-rich stars, models for the He enrichment that would involve spherically symmetrical mass loss. It immediately imposes the constraint that the He enrichment occurs where the mass loss is reduced below its average value, presumably because of horizontal magnetic fields.

In this section we define a model to study how the separation calculations presented above constrain realistic models for main-sequence He-rich stars. Because of the observational evidence presented by Barker *et al.* (1982), we assume that both magnetic fields and mass loss are involved and try to determine how one influences the other. We assume that magnetic fields can be represented by the dipole plus quadrupole configuration as presented by Michaud, Mégessier, and Charland (1981; see their Fig. 1). These seem sufficient to reproduce the observed magnetic field variations. For most cases that have been studied, the quadrupole configuration is of the order of 50% that of the dipole. Then the field lines are open at both poles but closed elsewhere. They are parallel to the surface on a ring shifted from the equator toward the strong pole.

Mass loss can most easily occur where the field lines are vertical, that is, where the magnetic field has no effect on vertical motion. Since to obtain He overabundances by diffusion requires mass loss, it is natural to assume that the He overabundance should be concentrated at the poles. It is then surprising that the He abundance shows a single wave pattern: since the maximum mass-loss rate can occur at both poles, one would expect to see a He-rich patch as each pole appears on the surface of the star, but only one maximum appears each period.

It was shown in § II that the mass-loss rate had to be at least $5 \times 10^{-12}\ M_\odot\ {\rm yr}^{-1}$ to explain the observed line asymmetries. If one assumes that this mass loss must be concentrated close to the poles, it reduces the surface over which the mass loss occurs and so increases the local mass-loss rate, so that at the poles it needs to be even larger. The enrichment by diffusion requires that the mass-loss rate be no larger than $10^{-12}\ M_\odot\ {\rm yr}^{-1}$ where the enrichment occurs. *Most of the mass loss must therefore take place where there is no He enrichment.* This leads us to assume that most of the mass loss occurs at the poles but that the He enrichment takes place where the magnetic field is horizontal or at intermediate locations.

That the He enrichment must occur where the mass-loss rate is attenuated implies that it must be centered where the magntic field is horizontal, presumably in a ring. Such configurations have been studied by Michaud, Mégessier, and Charland (1981) and have been shown to lead to time variations of equivalent widths that have either one or two maxima during each period (see their Figs. 5 and 7) depending on the exact parameters. Even when two maxima are present, they are often undistinguishable from a single maximum at the accuracy of the measurements. The maximum furthermore occurs in phase with the strong magnetic pole, as is observed to be the case here. The double maximum is unrealistically emphasized in the results of Michaud *et al.* by their assumption that the element of interest is entirely concentrated in the ring and is absent outside of it. The single maximum in each phase that is observed for He can be simply explained by the concentration of He in a single ring, as seems required by the reduction of the mass loss needed to permit the He enrichment by diffusion.

Detailed models of the interaction between magnetic fields and mass loss do not exist. Michaud, Mégessier, and Charland (1981) assume that the density structure of the outer atmosphere is not modified by mass loss. This is clearly not applicable here. Because mass-loss rates of the order of $10^{-12}\ M_\odot\ {\rm yr}^{-1}$ are involved, it is easy to verify that the low-density region of the atmosphere is rapidly modified by the outgoing gas. If the magnetic field starts slowing down diffusion at $\tau = 0.01$, as is the case if the outer atmosphere is not modified by mass loss, the total mass above that point is at most 0.1 g cm^{-2} or $2 \times 10^{-11}\ M_\odot$. It takes less than 10^2 yr to double this mass if a wind of $10^{-12}\ M_\odot\ {\rm yr}^{-1}$ accumulates without leaving the star. Within that time, the density increases in the magnetosphere and the wind accumulates where the magnetic field prevents it from leaving the star. It accumulates until either the density is large enough so that diffusion across the field lines is large or until the field lines break because the magnetic pressure is not large enough to contain the gas. A detailed study of how this occurs is needed but is outside the scope of the present paper. Some aspects of this process have been studied by Havnes and Goertz (1984), but they did not consider that the main driving of the mass loss can be radiative pressure and

that the mass loss then needs to be suppressed close to the star by magnetic fields. One needs to determine how the mass-loss rate is modified by the inclination of the magnetic field (Bolton 1984). Friend and MacGregor (1984) only considered the effect of open magnetic field lines on the mass loss and so could not determine how the magnetic field slows down diffusion.

Further observations of He-rich stars should also put interesting constraints on models of radiatively driven mass loss. Abbott (1979) has obtained the result that above $T_{\rm eff} = 25{,}000$ K winds were self-initiating, while between 14,000 and 25,000 K both static solutions and wind solutions existed. How strongly the mass-loss rates observed on He-rich stars follow the extrapolation of the mass-loss rates determined at higher temperatures will better determine the low-temperature limit of the radiatively driven winds and the effect of magnetic fields in controlling such winds. It may well be that below 25,000 K mass-loss rates decrease more rapidly than at higher $T_{\rm eff}$ but do not disappear suddenly.

The model that assumes separation to occur in the atmosphere, as originally suggested by Vauclair (1975), has at least two important observational consequences. The first one is the $T_{\rm eff}$ dependence of the mass loss that leads to He overabundances. As seen in § V*d*, the mass-loss rate must be smaller (by a factor of 3–10) in the hotter stars than in the cooler stars for this process to work. This is surprising, since the mass-loss rate increases very rapidly with $T_{\rm eff}$ if it is driven by radiation pressure. The empirical mass-loss formula of Abbott (1982) leads to a mass-loss rate proportional approximately to $T_{\rm eff}^7$. In the regions where there are He overabundances, this trend must be reversed completely if the overabundances are to be explained by chemical separation in the atmosphere.

The abundances of heavy elements permit another observational test. In those He-rich stars where the mass-loss rate is largest at the magnetic poles and smaller elsewhere, the mass-loss rate is everywhere at least $10^{-12}\ M_\odot\ {\rm yr}^{-1}$, and there can be *no* anomaly of an ionized element; in particular, there can be no abundance anomaly of the CNO elements. The downward diffusion velocity of heavy elements would be smaller than that of helium, since the heavy elements would be ionized while helium is still neutral. The diffusion coefficient of neutral atoms is 100 times larger than for ionized atoms (Michaud, Martel, and Ratel 1978), and this leads to the diffusion velocity of C being 30 times smaller than that of He. Diffusion then leads to normal abundances for CNO, at least in those cases where He is neutral, that is, in the cooler of the He-rich stars. This suggests an interesting observational test, since, if the He overabundance is caused by nuclear reactions, the abundances of CNO should be modified. In these stars hydrogen burning goes through the CNO cycle and concentrates the original C and O abundances in N. The N abundance maximum should furthermore be in phase with the He maximum abundance in any nuclear physics–based model, while the C and O abundances should vary in antiphase. Such a change cannot occur if the He overabundance is caused by separation in the atmosphere.

The remarks made above on the location of He enhancement further lead us to conclude that the CNO abundances must be normal over the whole stellar surface. Since the mass-loss rate is expected to be larger at the poles, of order of $10^{-11}\ M_\odot\ {\rm yr}^{-1}$, there will be no separation of CNO there either. There cannot be, where the He enrichment is concentrated, and so no modification of CNO abundances is expected in this model anywhere on the surface. It should be possible to test this conclusion observationally. Note that Hunger (1986) concludes that the CNO abundances are essentially normal in the He-rich stars where they have been determined with enough accuracy. Hardorp *et al.* (1986) had no He-rich stars in their sample of main-sequence B stars for which they determined C and N abundances.

In their outer regions, He-rich stars have a He convection zone. It starts at an optical depth of 2 or 3 and ends at an optical depth of 30. It is due to He II ionization. It cannot disappear by He settling at its bottom because the mass-loss rate is too large (see Fig. 5) to allow He settling. Some atmosphere models also have convection zones due to He I ionization at optical depths that are smaller than unity (see, e.g., Mihalas 1965). Given the high velocity of random motions in convection zones, these are nearly certainly homogeneous (Schatzman 1969). The separation cannot take place in convection zones. It is also believed that convection zones lead to some overshooting (Latour, Toomre, and Zahn 1981). In the presence of such convection zones, can separation take place in the atmosphere of He-rich stars? The He separation can only start where overshooting is stabilized and the atmosphere is stable. Perhaps the magnetic field could eliminate the convection or at least the overshooting in parts of the surface. If, because of overshooting, the atmosphere were mixed, the separation could only take place in the wind. Abundance anomalies of CNO are then possible. Determining observationally where the separation takes place determines whether and where the magnetic field has been able to suppress the convection efficiently.

The greatest uncertainty in this discussion is probably related to the determination of the mass-loss rate. If there are stars that lose mass at a smaller rate than the rate implied by the asymmetries of HD 184927 (see § II) and still develop He overabundances, it is possible that the overabundances would develop at the pole if the total mass-loss rate for the star were less than $10^{-12}\ M_\odot\ {\rm yr}^{-1}$. Then the mass-loss rate where the magnetic field lines are horizontal would be smaller than at the poles and could be small enough to allow anomalies of heavy elements. This would, however, be possible only if the mass-loss rate were at most $10^{-13}\ M_\odot\ {\rm yr}^{-1}$ there. Future observations of line asymmetries in He-rich stars of various temperatures should clarify the situation.

In this paper, the effect of diffusion on the mechanism by which the wind is accelerated has not been discussed. In the He-rich stars of the upper main sequence, radiation pressure through the lines of heavy elements is probably the main acceleration mechanism (Abbott 1982; Lucy and Solomon 1970). Heavy elements absorb the momentum from the photons, and they must transfer it to H and He. This transfer is done by the same process which gives the friction coefficient of equation (8). Slipping should then start occurring between heavy elements and H or He at about the same mass-loss rate as found above between H and He. Presumably this could lead to a more abrupt decrease of the mass-loss rate with luminosity at about the mass-loss rate where He enrichment by the wind can start occurring. Helium is harder to drag along than H, since it is 4 times heavier, but this is compensated by the factor of 4 increase of the drag coefficient when He is twice ionized. However, since they constitute only about 2% of the total

mass, heavy elements must transfer to H and He 50 times the momentum they need for their own acceleration. This requires stronger coupling than that between H and He. On the other hand, the friction coefficient will depend on the state of ionization of individual elements. These aspects of the problem are essential to determine quantitatively the effect of diffusion on the acceleration mechanism. They will be discussed in a forthcoming paper by Michaud and Fakir (1987).

The authors thank Professor Leon Mestel for useful discussions on wind theory.

REFERENCES

Abbott, D. C 1979, in *IAU Symposium 83, Mass Loss and the Evolution of O Type Stars*, ed. P. S. Conti and C. W. H. de Loore (Dordrecht: Reidel), p. 237.
———. 1982, *Ap. J.*, **259**, 282.
Barker, P. K., Brown, D. N., Bolton, C. T., and Landstreet, J. D. 1982, in *Advances in Ultraviolet Astronomy: Four Years of IUE Research* (NASA CP-2238), p. 589.
Bolton, C. T. 1984, in *Proc. HVAR Workshop on Rapid Variability of Early-Type Stars* (Harvard Obs. Bull. 7, 241).
Borra, E. F., and Landstreet, J. D. 1979, *Ap. J.*, **228**, 809.
Bruhweiler, F. C., and Kondo, Y. 1983, *Ap. J.*, **269**, 657.
Burgi, A., and Geiss, J. 1986, *Solar Phys.*, **103**, 347.
Castor, J. I. 1986, *Pub. A.S.P.*, **98**, 52.
Castor, J. I., Lutz, J. H., and Seaton, M. J. 1981, *M.N.R.A.S.*, **194**, 547.
Cesarsky, C. J., and Montmerle, T. 1983, *Space Sci. Rev.*, **36**, 173.
Chapman, S., and Cowling, T. G. 1970, *The Mathematical Theory of Non-uniform Gases* (3d ed.; Cambridge: Cambridge University Press).
Cuperman, S., and Metzler, N. 1975, *Ap. J.*, **196**, 205.
Delache, P. 1967, *Ann. d'Ap.*, **30**, 827.
Friend, D. B., and MacGregor, K. B. 1984, *Ap. J.*, **282**, 591.
Geiss, J. 1982, *Space Sci Rev.*, **33**, 201.
Geiss, J., Hirt, P., and Leutwyler, H. 1970, *Solar Phys.*, **12**, 458.
Hardorp, J., Cugier, H., Koratkar, A., and Scott, J. 1986, in *Joint NASA/ESA/SERC Conf., University College London* (ESA SP-263), p. 377.
Havnes, O., and Goertz, C. K. 1984, *Astr. Ap.*, **138**, 421.
Heber, U. 1986, *Astr. Ap.*, **155**, 33.
Hollweg, J. V. 1981, *J. Geophys. Res.*, **86**, 8899.
Hunger, K. 1986, in *IAU Colloquium 87, Hydrogen Deficient Stars and Related Objects*, ed. K. Hunger, D. Schönberner, and N. K. Rao (Dordrecht: Reidel), p. 261.
Jokipii, J. R. 1966, in *The Solar Wind*, ed. R. J. Makin and Neugebauer (New York: Pergamon), p. 215.
Joselyn, J., and Holzer, T. E. 1978, *J. Geophys. Res.*, **83**, 1019.
Latour, J., Toomre, J., and Zahn, J.-P. 1981, *Ap. J.*, **248**, 1081.
Lucy, L. B. 1982, *Ap. J.*, **255**, 286.
Lucy, L. B., and Solomon, P. 1970, *Ap. J.*, **159**, 879.
Lucy, L. B., and White, R. L. 1980, *Ap. J.*, **241**, 300.
Meyer, J. P. 1985, *Ap. J. Suppl.*, **57**, 173.
Michaud, G., and Charland, Y. 1986, *Ap. J.*, **311**, 326.
Michaud, G., and Fakir, R. 1987, in preparation.
Michaud, G., Martel, A., and Ratel, A. 1978, *Ap. J.*, **226**, 483.
Michaud, G., Mégessier, C., and Charland, Y. 1981, *Astr. Ap.*, **103**, 244.
Michaud, G., Montmerle, T., Cox, A. N., Magee, N. H., Hodson, S. W., and Martel, A. 1979, *Ap. J.*, **234**, 206.
Mihalas, D. 1965. *Ap. J. Suppl.*, **9**, 321.
———. 1972, *NCAR Technical Note NCAR-TN/STR-76* (Boulder: National Center for Atmospheric Research).
Montmerle, T. 1984, *Adv. Space Res.*, **4**, 357.
Montmerle, T., and Michaud, G. 1976, *Ap. J. Suppl.*, **31**, 489.
Nakada, M. P. 1969, *Solar Phys.*, **7**, 302.
———. 1970, *Solar Phys.*, **14**, 475.
Osmer, P. S., and Peterson, D. 1974, *Ap. J.*, **187**, 117.
Pelletier, C., Fontaine, G., Wesemael, F., Michaud, G., and Wegner, G. 1986, *Ap. J.*, **307**, 242.
Peterson, D. M., and Theys, J. C. 1981, *Ap. J.*, **244**, 947.
Petre, R., Shipman, H. L., and Canizares, C. R. 1986, *Ap. J.*, **304**, 356.
Schatzman, E. 1969, *Astr. Ap.*, **3**, 331.
Vauclair, S. 1975, *Astr. Ap.*, **45**, 233.
———. 1981, *A.J.*, **86**, 513.
Vauclair, S., Hardorp, J., and Peterson, D. A. 1979, *Ap. J.*, **227**, 526.
Vauclair, S., and Meyer, J. P. 1985, *Proc. 19th Internat. Cosmic Ray Conf.*, Vol. 4, ed. F. C. Jones, J. Adams, and G. M. Mason (NASA CP-2376), p. 233.
Wesemael, F., Auer, L. H., Van Horn, H. M., and Savedoff, M. P. 1980, *Ap. J. Suppl.*, **43**, 159.
Wesemael, F., Green, R. F., and Liebert, J. 1985, *Ap. J. Suppl.*, **58**, 379.
White, R. L. 1985, *Ap. J.*, **289**, 698,
Yeh, T. 1970, *Planet. Space Sci.*, **18**, 199.

J. DUPUIS, G. FONTAINE, and G. MICHAUD: Département de Physique, Université de Montréal, C.P. 6128, succursale A, Montréal, Québec, Canada J3C 3J7

T. MONTMERLE: DPh/EP/Ap, CEN Saclay, 91191 Gif-sur-Yvette Cedex, France